Full confirmation of icosahedral Bose-Einstein statistics in cold ¹²C₆₀

Ya-Chu Chan, 1,2 Lee R. Liu, 1,3,* Andrew Scheck, 1,3 David J. Nesbitt, 1,2,3 Jun Ye, 1,3,† and Dina Rosenberg, 1,3 ¹JILA, National Institute of Standards and Technology and University of Colorado, Boulder, Boulder, Colorado 80309, USA ²Department of Chemistry, University of Colorado, Boulder, Boulder, Colorado 80309, USA ³Department of Physics, University of Colorado, Boulder, Boulder, Colorado 80309, USA

(Received 19 June 2024; accepted 17 June 2025; published 7 August 2025)

The quantum mechanical nature of high icosahedral symmetry, spherical top molecules, such as ¹²C₆₀, is particularly evident at low total angular momentum quantum number J. However, the small rotational constant of such large molecules leads to the most populated levels having hundreds of rotational quanta even at modest temperatures, making transitions from low-J states challenging to observe. We combine a laser desorption C₆₀ source with helium buffer gas cooling to achieve the lowest temperature of 30 K to date, enabling the observation of R(J < 30) in the 8.4 μ m rovibrational band of $^{12}C_{60}$. Based on the absence of 15 transitions due to the exchange statistics of 60 identical spin-0 nuclei, we place an upper limit of $1.4(5) \times 10^{-8}$ on possible violations of the Bose-Einstein statistics, offering improvements over previous studies that considered only one missing line in molecular systems with two identical bosonic nuclei (e.g., ¹⁶O₂ and ¹²C ¹⁶O₂).

DOI: 10.1103/3fjd-lwkd

Strong intramolecular interactions and long-lived rotational and vibrational degrees of freedom make large molecules interesting and complementary platforms for probing strongly correlated many-body phenomena [1,2] and quantum information processing [3-5]. Rovibrational spectroscopy provides one powerful key to unlock these capabilities. Molecules beyond ~ 10 atoms, however, typically exhibit intrinsic spectral congestion in the infrared bands due to the rapidly increasing vibrational density of states with increasing energy and atom number [6,7]. ¹²C₆₀ is a notable exception: Due to its rigidity and rare icosahedral symmetry, it is the largest gas-phase molecule for which full quantum state resolution in the infrared has been achieved to date [8].

A series of high-resolution spectroscopic measurements have provided further understanding of the structure and dynamics of individual C₆₀ molecules [8], including the intramolecular energy relaxation pathways [9] and the ergodicity breaking observed in the rotational fine structure [1]. These results were obtained using a 900 K oven source coupled to a liquid nitrogen-cooled buffer gas cell [6,10,11]. However, significant heat load from the oven constrained the cell temperature to \sim 140 K or higher, restricting observation to rovibrational transitions from states of high total angular momentum quantum number $(J \ge 63)$ due to the formidable rotational partition function of C₆₀ [8]. While nuclear spin intensity alternation was reported in Ref. [8], the complete

Published by the American Physical Society under the terms of the Creative Commons Attribution 4.0 International license. Further distribution of this work must maintain attribution to the author(s) and the published article's title, journal citation, and DOI.

disappearance of rovibrational transitions, arising from the exchange statistics of 60 identical spin-0 ¹²C nuclei, only happens for specific J < 30 levels in the vibrational ground state [12,13]. Observing these striking quantum mechanical effects therefore requires a significant concentration of populations into the lower-J states, which can only be achieved through reducing the temperature.

An alternative method to produce gas-phase C₆₀ with a vastly reduced heat load is through laser desorption. Vaporization of solid C₆₀ targets with pulsed lasers has been demonstrated to generate C₆₀ molecules with little fragmentation [14,15]. To cool laser-desorbed C₆₀, Haufler et al. coupled this technique to a supersonic beam source operating at a high helium backing pressure of 10 atm [16]. Through $\sim 10^5$ collisions with He, reduced vibrational hot bands were observed in the ultraviolet photoelectron spectra. In this Letter, we build on existing laser desorption techniques and combine them with a cryogenic cell to cool C_{60} through $\!\geqslant\!10^6$ collisions with cold helium buffer gas, achieving a record-low temperature of 30 K. Quantum state resolved infrared spectroscopy of C₆₀ enables quantitative characterization of translational, vibrational, and rotational temperatures. With an order of magnitude increase in low-J populations, R-branch rotational progressions from J < 30 levels are measured for the first time, revealing the absence of certain transitions predicted by nuclear spin statistics. The simultaneous observation of 15 missing lines imposes a tight bound on possible violations of the icosahedral Bose-Einstein statistics.

The experimental apparatus is illustrated in Fig. 1. A continuous-wave 532 nm laser with a 2 to 3.5 W peak power and a pulse duration of 200 ms, controlled by an acousto-optic modulator, is focused onto 5- to 10-µm-thick C₆₀ film targets and produces desorption spot sizes of 300 to 450 µm. The desorbed C₆₀ molecules enter a buffer gas cell filled with helium. For the 77 K and 10 K setups, the cell is anchored

^{*}Contact author: lee.richard.liu@gmail.com [†]Contact author: ye@jila.colorado.edu

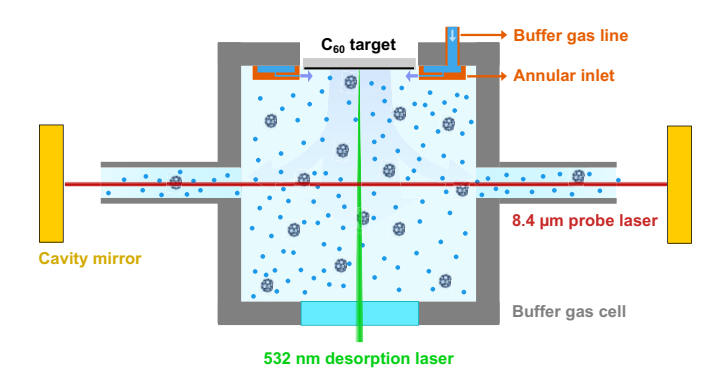


FIG. 1. A schematic of the laser desorption and buffer gas cooling apparatus (not to scale). The C_{60} film target is positioned at the center of an annular inlet, through which He flow is introduced. A 532 nm desorption laser (green) is rastered across the target, and the desorbed C_{60} molecules cool via collisions with cold buffer gas. The 8.4 µm probe laser (red) is coupled into a high-finesse cavity ($\mathcal{F}=12\,000$) to enhance the absorption path length. Tubings along the cavity axis allow the passage of the probe laser while maintaining a high buffer gas density inside the $6\times 6\times 6$ cm³ cell: 12.5 mm diameter $\times 10$ mm length (77 K setup) and 6.5 mm diameter $\times 25$ mm length (10 K setup).

to a liquid nitrogen Dewar or a helium cryostat, respectively. In the cryostat setup, charcoal shields mounted on the 10 K stage are used to pump helium in addition to a turbopump. Note that the use of a helium cryostat is enabled by (1) the 1000-fold reduction in heat load of laser desorption compared to an oven and (2) relatively efficient translational/rotational cooling of C_{60} in He buffer gas [17].

To characterize the shot-to-shot uniformity of laserdesorbed C₆₀, we record the absorption of the probe laser at 1184.8524 cm⁻¹, corresponding to the Q branch band head in the 8.4 µm fundamental band [8]. Sample results for the 10 K setup are shown in Fig. 2(a). Remarkably, the measured absorption, which is proportional to the C₆₀ density, only fluctuates by less than 10% from shot to shot. Next, we acquire absorption spectra in the R branch ($\Delta J = +1$) region by scanning the probe laser frequency over 130 MHz during the 50 ms window depicted in Fig. 2(a), over which the C_{60} density remains stable. After shutting off the desorption laser, C₆₀ density drops to zero in less than 10 ms, and a subsequent "empty cavity" spectrum is recorded. These two consecutive spectra [Fig. 2(b)] allow the subtraction of slow intensity fluctuations such as those due to parasitic etalon fringes, revealing weak C_{60} absorptions. As shown in Fig. 2(c), the R(6) transition is observed with a linewidth of ~ 9 MHz.

Resolving the rovibrational transitions indicates that cold C_{60} molecules are produced. To characterize the translational, vibrational, and rotational temperatures, several fully resolved R-branch transitions are measured, with experimental spectra shown in Fig. 3(a). From the populations per J multiplet component, rotational temperatures of 94(4) K and 30(1) K are determined for the 77 K and 10 K setups, respectively [17]. Good agreement between the experimental and theoretical intensities is attributed to the reproducibility of the laser desorption source. The characteristic icosahedral nuclear spin intensity alternation (e.g., the 2:1 and 3:2 intensity ratios for

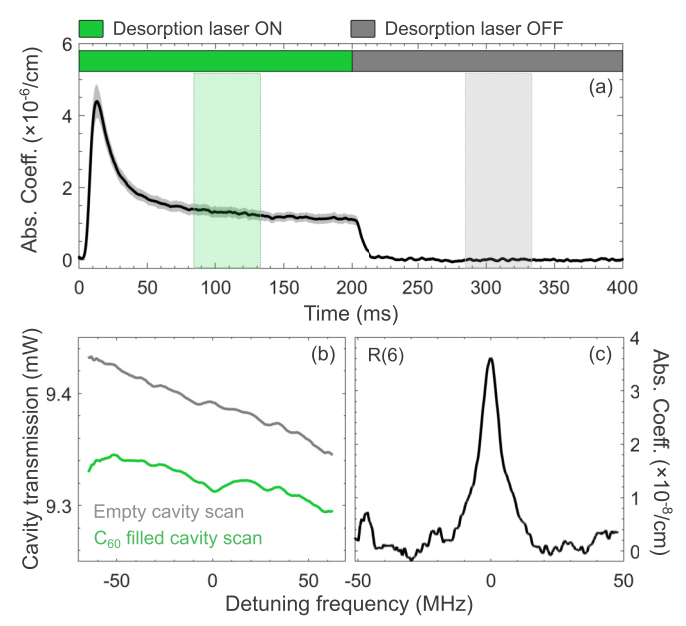


FIG. 2. (a) Absorption at 1184.8524 cm $^{-1}$ is monitored as the desorption laser is alternately pulsed on and off. The black trace shows the average over 40 shots, while the gray error band indicates the shot-to-shot standard deviation. (b) The 8.4 μ m laser is scanned around R(6) during the 50 ms windows depicted by translucent green and gray boxes in (a), yielding "C₆₀ filled" and "empty cavity" spectra. The data is averaged over 800 shots. An overall decrease in transmission is found in the C₆₀ filled spectra, likely arising from vibrationally hot C₆₀ with broad, continuous spectral features [8]. (c) R(6) absorption spectrum obtained by subtracting C₆₀ filled cavity transmission from empty cavity transmission, with the sloping baseline due to vibrationally hot C₆₀ further removed.

R(36):R(35) and R(66):R(65)) becomes more obvious under the colder 30 K conditions (*vide infra*).

The experimental line shapes for R(126) are presented in Fig. 3(b), with linewidths of 17(1) MHz and 14(1) MHz for the 77 K and 10 K setups, respectively. While the line shape measured with the liquid nitrogen Dewar setup resembles a Voigt profile, the spectrum obtained using the cryostat apparatus shows a sharper peak with humps on both sides, which is more evident in R(6) [Fig. 2(c)]. The humps arise from the hydrodynamic boost of the C_{60} /He mixture [11,18,19], by which the mean outward velocity is enhanced as the mixture is pumped out of the cell through the tubings (Fig. 1). The increase in the velocity along the probe laser axis results in equal blue/red Doppler shifts. Such hydrodynamic acceleration effects are supported by the short residence time of C₆₀ in the cell (5 ms for the 10 K setup, as shown in Fig. 2(a), and 9 ms for the 77 K setup), compared to the diffusion-limited lifetimes (10² to 10³ ms at helium densities of \sim 10¹⁶ cm⁻³) [20,21]. To incorporate this effect, the experimental line shape is fitted with three Voigt profiles [Fig. 3(b)]: One nonshifted Voigt, representing C₆₀ molecules not fully entrained in the helium flow, and two Doppler-shifted Voigts, constrained to have equal amplitudes but opposite signs for the frequency offsets.

A global fit is performed on all R(J) transitions [17], yielding Doppler linewidths of 8.5(9) and 5.7(6) MHz for the

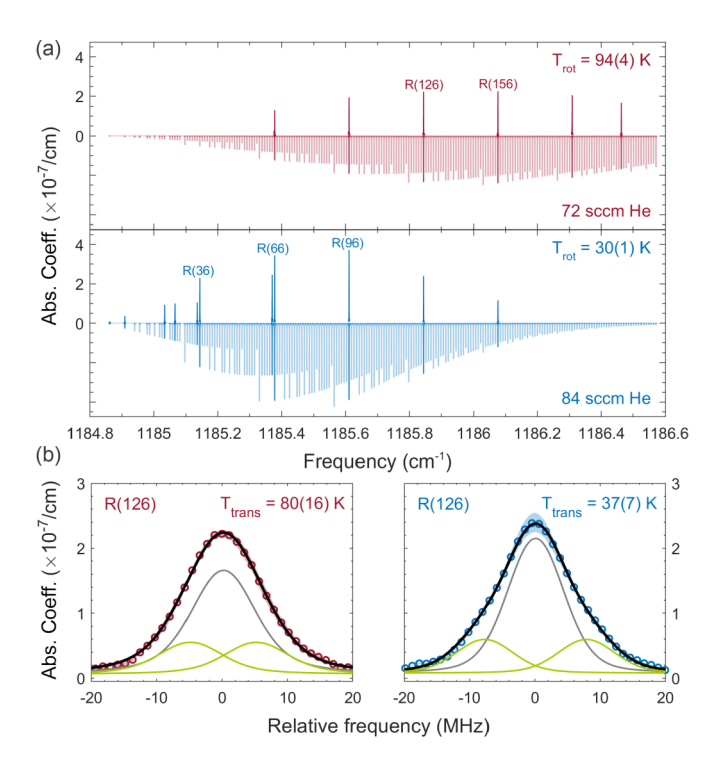


FIG. 3. Rotational and Doppler thermometry of laser-desorbed C_{60} in He buffer gas. (a) Experimental spectra measured with the 77 K (top, red) and 10 K setups (bottom, blue). Simulated spectra are inverted for clarity. The stepwise intensity modulation arises from icosahedral nuclear spin statistics. Rotational temperatures of 94(4) and 30(1) K are obtained from Boltzmann analysis. (b) Experimental line shapes (empty circles) of R(126) measured with the 77 K (left, red) and 10 K (right, blue) setups are averaged over 300 shots. Color bands represent the standard deviation. Black traces are fits to Voigt profiles including hydrodynamic effects, which are the sum of nonshifted (gray) and Doppler-shifted (green) Voigts. Translational temperatures of 80(16) K and 37(7) K are extracted from the Doppler linewidths.

77 K and 10 K setups, corresponding to translational temperatures of 80(16) K and 37(7) K, respectively. Hydrodynamic velocities of 43(4) m/s (77 K setup) and 66(7) m/s (10 K setup) are extracted from the fitted Doppler shifts. These are much lower than the terminal velocity of a He supersonic expansion (558 m/s), due to the velocity slip between the heavy C_{60} molecules and the light helium atoms [22,23], but are slightly higher than the mean velocity of a C₆₀ effusive source (23 m/s) at 30 K. The cryostat apparatus shows a higher hydrodynamic velocity due to the high charcoal pumping speed and lower tubing conductance, leading to a greater pressure difference between the cell ($\sim 10^{-1}$ Torr) and the chamber ($\sim 10^{-3}$ Torr). By way of contrast, the differential pressures for the 77 K setup are an order of magnitude smaller due to the larger aperture (12.5 mm vs. 6.5 mm for the 10 K setup, Fig. 1), yet it entrains a higher fraction of C₆₀ (38% compared to 25% for the 10 K setup) in the helium

Although we do not have high-resolution spectra for the vibrational hot bands, the vibrational temperature can be estimated from the fraction of laser-desorbed C_{60} in the vibrational ground state. Using the integrated intensity of the

8.4 µm band [24,25], the effective path length, the residence time of C₆₀ in the cell, and the cell volume, a total of $6.5(14) \times 10^{13}$ (77 K setup) and $9.8(21) \times 10^{13}$ (10 K setup) vibrational ground-state $^{12}C_{60}$ molecules are observed per 200 ms laser pulse [17]. This $^{12}C_{60}$ count can be ratioed with the total number of desorbed ¹²C₆₀, computed from the desorption spot size and film thickness to be $2.6(2) \times 10^{14}$ and $1.2(1) \times 10^{15}$ for the 77 K and 10 K setups, respectively. The resulting fraction of ¹²C₆₀ in the vibrational ground state is 25(6)% for the liquid nitrogen Dewar setup and 8(2)% for the cryostat apparatus as the lower bound. Comparison of these ratios to the probability of C₆₀ being in the vibrational ground state yields vibrational temperatures of ≤170 K (77 K setup) and $\leq 200 \,\mathrm{K}$ (10 K setup) [17]. These represent upper limits since not all the film may desorb as monomeric C_{60} . In addition, some C₆₀ molecules are impeded from entering the cell due to the buffer gas flow, while others impact and freeze on the wall before reaching the probe laser. Accounting for these factors should yield a lower vibrational temperature.

The experimentally determined translational and rotational temperatures agree within error bars, indicating that these degrees of freedom are nearly thermalized with each other and the buffer gas [17]. This is reasonable since translational and rotational thermalization typically occurs in less than one hundred collisions [26], or a duration of a few microseconds under our experimental conditions, which is three orders of magnitude shorter than the time it takes for C₆₀ to reach the probe laser (\sim 10 ms). Compared to translation and rotation, vibrationally inelastic collisions with He are far less efficient [26]. As a result, an experimental upper limit of \sim 200 K for the vibrational temperature is not unreasonable. Vibrational cooling of C₆₀ in a cryogenic cell proceeds by collisionally transferring its vibrational energy to the translational energy of helium buffer gas. Consequently, the extent of cooling depends largely on the number of collisions. While vibrational thermalization may occur rapidly in large molecules even from weak collisions due to efficient intramolecular vibrational redistribution (IVR) [27-30], the bottleneck is the energy transfer out of the lowest-frequency vibrations, with the probability decreasing exponentially with increasing energy gap [31]. Therefore, large molecules with softer vibrational modes are likely to quench more effectively [32]. Small molecules, in contrast, are expected to exhibit much less efficient quenching due to larger energy gaps and a much lower density of vibrational states [33,34].

Efficient vibrational cooling of large polycyclic aromatic hydrocarbons, such as ovalene ($C_{32}H_{14}$), has been demonstrated using a pinhole supersonic expansion, where a vibrational temperature of $\leq 100\,\mathrm{K}$ was achieved after 600 collisions with heavy rare gases [35]. Nevertheless, Stewart *et al.* showed that vibrational cooling of C_{60} was surprisingly insufficient in a slit jet supersonic expansion of Ar even at a backing pressure of $\sim 3\,\mathrm{atm}$, which resulted in 4000 collisions [36]. The lack of vibrational cooling was attributed to the rigidity of C_{60} , leading to a lowest-frequency vibration of 260 cm⁻¹, which is relatively high compared to molecules of similar size (e.g., 61 cm⁻¹ for ovalene). Our previous attempts with the oven source also showed inefficient vibrational cooling of C_{60} in helium buffer gas [8,9], which was likely due to the higher thermal conductivity of He, exacerbating heat

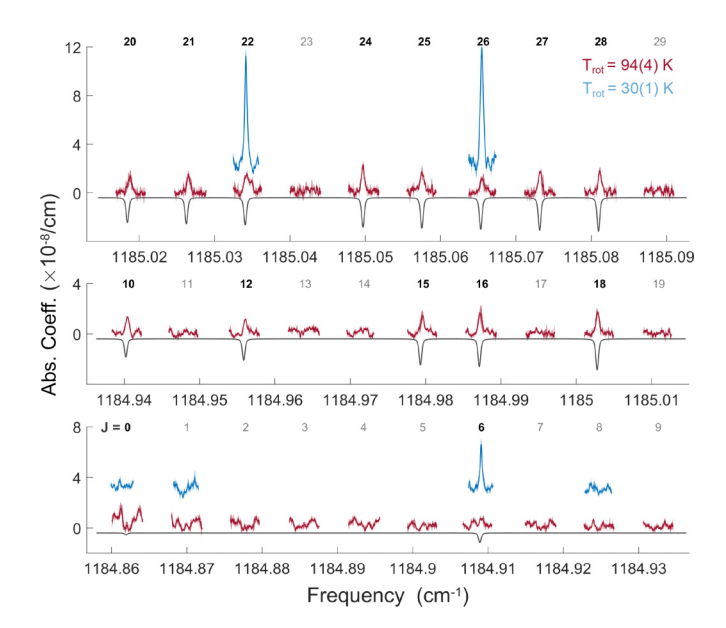


FIG. 4. R(J < 30) spectra in the 8.4 µm band of $^{12}C_{60}$. Experimental data are averaged over $\geqslant 200$ shots (red: 77 K setup, blue: 10 K setup, with spectra shifted upward for ease of comparison). The error bands (light red: 77 K setup, light blue: 10 K setup) represent the standard deviation. The simulated spectrum (gray, inverted) assumes a 94 K rotational temperature and includes icosahedral nuclear spin weights. The spectroscopic constants used in the simulation are determined from the high-J transitions in Ref. [8], which may lead to the observed discrepancies between the experimental and theoretical line centers for the low-J transitions.

transfer from the 1 kW oven to the cryogenic cell [17]. For our current 77 K setup, pressure in the cell is measured to be 265 mTorr at a He flow of 72 sccm, corresponding to a helium density of 3×10^{16} cm⁻³. For the 10 K setup, we can estimate a helium density of 7×10^{16} cm⁻³ from the pressure-broadening linewidths. Based on the buffer gas density, relative collision velocity, and elastic collision cross sections [9], a collision rate of $\sim 10^8 \text{ s}^{-1}$ between C₆₀ and He is computed. It takes approximately 10 ms for desorbed C₆₀ to reach the probe laser, leading to a total of 10⁶ collisions with cold He buffer gas. This number is three orders of magnitude higher than the slit supersonic beam experiment, highlighting the challenges in the vibrational cooling of large, rigid molecules. Lastly, the 10 K setup shows a smaller fraction of vibrationally cold C₆₀ and a higher upper limit for the vibrational temperature, consistent with the decrease in vibrational relaxation probability when colliding with slower-moving helium [37].

Of particular note, the reduced temperatures permit the observation of complete R(J < 30) progressions for the first time (Fig. 4). The characteristic $^{12}C_{60}$ intensity alternation demonstrates a striking example of nuclear spin statistics in a molecular system, arising from rigorous symmetry constraints on the total molecular wave function upon the exchange of identical nuclei. The classic example is hydrogen (H₂), where the total wave function must be antisymmetric with respect to the interchange of two fermionic H atoms, resulting in a 1:3 nuclear spin alternation between even:odd J levels. This effect can also lead to the complete disappearance of rotational states, such as the even J levels in the ground vibronic state

of oxygen with two spin-0 nuclei ($^{16}O_2$, $^3\Sigma_g^-$). Nuclear spin statistics become more complicated as the number of identical nuclei increases. For instance, methane ($^{12}CH_4$) has $2^4=16$ nuclear spin states, which are of A (meta, total nuclear spin I=2), F (ortho, I=1), and E (para, I=0) symmetries in the tetrahedral group and with statistical weights of 5, 9, and 2, respectively. Unlike diatomic molecules, each $J \ge 2$ rotational level in methane contains states of multiple nuclear spin species, due to the additional (2J+1)-fold K degeneracy (the projection of total angular momentum along the symmetry axis) in spherical top molecules.

¹²C₆₀ is also a spherical top, but with a much higher icosahedral (I_h) symmetry. The equivalence of all 60 atoms implied by the I_h symmetry was confirmed using 13 C nuclear magnetic resonance spectroscopy [38,39]. Because there is only one symmetric nuclear spin state with I=0, the allowed rovibrational states for $^{12}C_{60}$ must be of A_g symmetry in the I_h point group. For the ground states with J < 30, these correspond to the J = 0.6,10,12,15,16,18,20-22,24-28 levels (each with a statistical weight of 1), with the remaining states completely absent [13]. All $J \ge 30$ levels exist but with a statistical weight much less than the (2J + 1)-fold K degeneracy. On the other hand, the ¹³C₆₀ isotopomer has a total of 2^{60} nuclear spin states due to the 60 indistinguishable spin- $\frac{1}{2}$ fermions. There are no symmetry-forbidden J levels, and the derivation of statistical weights becomes significantly more complex [40]. In our 94 K spectra, the complete absence of R(J = 11,13,14,17,19,23,29), dictated by the nuclear spin statistics, is clearly evident. However, additional features are found around 1) R(J = 1-5,7-9), where transitions should not exist due to symmetry-forbidden lower states, and 2) R(J = 0.6,22,26), where only a single peak is expected. To understand the origin of these peaks, we record the spectra at a lower temperature of 30 K. While transitions from the symmetry-allowed J = 6,22,26 levels become stronger, the magnitudes of additional features decrease or completely vanish. If we assume them to be at the noise level in the 30 K spectra, then based on the expected temperature-dependent intensity ratios, additional peaks in the 94 K spectra likely reflect the high-J ($J \ge 130$) transitions. While we cannot unambiguously assign them at this stage, they potentially arise from (1) nearby Q branch, (2) dark states, (3) C₆₀ isotopologues, and/or (4) vibrational hot bands.

Lastly, the permutations of 60 identical bosonic nuclei in ¹²C₆₀ provide a unique platform to test the symmetrization postulate and the spin-statistics connection [41], which dictate that the only possible states of a system containing identical particles must be either all symmetric or all antisymmetric and that bosons follow Bose-Einstein statistics while fermions obey Fermi-Dirac statistics. However, quantum mechanics would also permit more complicated symmetries, and theories allowing small deviations from conventional statistics have been proposed [42–45]. Rovibrational spectra of $^{12}C_{60}$ offer a direct and quantitative method to probe and/or set upper limits on such violations. By calculating the probability of simultaneously observing 15 missing lines in the R(J < 30) progressions (i.e., finding states that do not follow Bose-Einstein statistics), based on the expected signal-tonoise ratios, an upper bound of $1.4(5) \times 10^{-8}$ is established for possible violations of the spin-statistics connection [17]. The detection of multiple missing lines significantly enhances sensitivity to small violations of quantum statistics, offering improvements over previous tests with $^{16}O_2$ and $^{12}C^{16}O_2$ [46–51], which considered only a single missing line, and highlights the potential of large molecules as a testbed for fundamental physics. Moreover, with more than two identical bosons, $^{12}C_{60}$ enables the search for states that are neither symmetric nor antisymmetric, providing a test of the symmetrization postulate [52].

In summary, we demonstrate efficient collisional cooling of laser-desorbed C_{60} with helium, achieving the lowest temperature of 30 K reported to date. The significant concentration of populations into the low-J levels allows the hitherto undetected R(J < 30) transitions to be observed, providing new tests of bosonic indistinguishability involving highly symmetric, large molecules. Finally, this approach can be directly applied to the production, cooling, and detection of other large molecules in the gas phase, enabling quantum state resolved spectroscopy of molecules with even higher density of states. Examples include $^{13}C_{60}$, which follows Fermi-Dirac

statistics and exhibits spin-rotational coupling, and C_{70} , a larger fullerene with a lower D_{5h} symmetry.

We thank Adam Ellzey for technical assistance; the COS-INC Fabrication facility at CU Boulder, particularly Dylan Bartusiak; and Jutta Toscano for the inspiration to pursue laser desorption of C₆₀. We thank Jacob Higgins and Baruch Margulis for providing useful comments on the manuscript. Funding support for this work is provided by AFOSR (Grant No. FA9550-19-1-0148); NSF QLCI (Grant No. QLCI OMA-2016244); NSF (Grant No. Phys-1734006); and NIST. Support is also acknowledged from the U.S. Department of Energy, Office of Science, National Quantum Information Science Research Centers, and Quantum Systems Accelerator. D.R. acknowledges support from the Israeli CHE Quantum Science fellowship, and is an awardee of the Weizmann Institute National Postdoctoral Award Program for Advancing Women in Science. Y.-C.C. and D.J.N. acknowledge support from DOE (Grant No. DE-FG02-09ER16021) and NSF (Grant No. CHE 2053117).

- [1] L. R. Liu, D. Rosenberg, P. B. Changala, P. J. Crowley, D. J. Nesbitt, N. Y. Yao, T. V. Tscherbul, and J. Ye, Ergodicity breaking in rapidly rotating C₆₀ fullerenes, Science 381, 778 (2023).
- [2] F. Schulz, M. Ijäs, R. Drost, S. K. Hämäläinen, A. Harju, A. P. Seitsonen, and P. Liljeroth, Many-body transitions in a single molecule visualized by scanning tunnelling microscopy, Nat. Phys. 11, 229 (2015).
- [3] R. Sawant, J. A. Blackmore, P. D. Gregory, J. Mur-Petit, D. Jaksch, J. Aldegunde, J. M. Hutson, M. R. Tarbutt, and S. L. Cornish, Ultracold polar molecules as qudits, New J. Phys. 22, 013027 (2020).
- [4] M. Zeppenfeld, A robust framework for quantum computation using quasi-hidden molecular degrees of freedom, arXiv:2311.14133 [physics.atom-ph].
- [5] V. V. Albert, E. Kubischta, M. Lemeshko, and L. R. Liu, Topology and entanglement of molecular phase space, arXiv:2403.04572 [quant-ph].
- [6] B. Spaun, P. B. Changala, D. Patterson, B. J. Bjork, O. H. Heckl, J. M. Doyle, and J. Ye, Continuous probing of cold complex molecules with infrared frequency comb spectroscopy, Nature (London) 533, 517 (2016).
- [7] P. B. Changala, B. Spaun, D. Patterson, J. M. Doyle, and J. Ye, Sensitivity and resolution in frequency comb spectroscopy of buffer gas cooled polyatomic molecules, Appl. Phys. B 122, 292 (2016).
- [8] P. B. Changala, M. L. Weichman, K. F. Lee, M. E. Fermann, and J. Ye, Rovibrational quantum state resolution of the C₆₀ fullerene, Science 363, 49 (2019).
- [9] L. R. Liu, P. B. Changala, M. L. Weichman, Q. Liang, J. Toscano, J. Kłos, S. Kotochigova, D. J. Nesbitt, and J. Ye, Collision-Induced C₆₀ Rovibrational Relaxation Probed by State-Resolved Nonlinear Spectroscopy, PRX Quantum 3, 030332 (2022).
- [10] J. D. Weinstein, R. deCarvalho, T. Guillet, B. Friedrich, and J. M. Doyle, Magnetic trapping of calcium monohydride

- molecules at millikelvin temperatures, Nature (London) **395**, 148 (1998).
- [11] D. Patterson and J. M. Doyle, Bright, Guided molecular beam with hydrodynamic enhancement, J. Chem. Phys. **126**, 154307 (2007).
- [12] W. G. Harter and T. C. Reimer, Nuclear spin weights and gas phase spectral structure of ¹²C₆₀ and ¹³C₆₀ buckminsterfullerene, Chem. Phys. Lett. **194**, 230 (1992).
- [13] P. R. Bunker and P. Jensen, Spherical top molecules and the molecular symmetry group, Mol. Phys. 97, 255 (1999).
- [14] G. Meijer and D. S. Bethune, Laser deposition of carbon clusters on surfaces: A new approach to the study of fullerenes, J. Chem. Phys. **93**, 7800 (1990).
- [15] H. Ajie, M. M. Alvarez, S. J. Anz, R. D. Beck, F. Diederich, K. Fostiropoulos, D. R. Huffman, W. Kraetschmer, Y. Rubin et al., Characterization of the soluble all-carbon molecules C₆₀ and C₇₀, J. Phys. Chem. 94, 8630 (1990).
- [16] R. Haufler, L.-S. Wang, L. Chibante, C. Jin, J. Conceicao, Y. Chai, and R. Smalley, Fullerene triplet state production and decay: R2PI probes of C₆₀ and C₇₀ in a supersonic beam, Chem. Phys. Lett. 179, 449 (1991).
- [17] See Supplemental Material at http://link.aps.org/supplemental/ 10.1103/3fjd-lwkd for discussions on translational, rotational, and vibrational thermometry; C_{60} thermalization; and nuclear spin statistics of C_{60} .
- [18] S. E. Maxwell, N. Brahms, R. deCarvalho, D. R. Glenn, J. Helton, S. V. Nguyen, D. Patterson, J. Petricka, D. DeMille, and J. M. Doyle, High-flux beam source for cold, slow atoms or molecules, Phys. Rev. Lett. 95, 173201 (2005).
- [19] N. R. Hutzler, M. F. Parsons, Y. V. Gurevich, P. W. Hess, E. Petrik, B. Spaun, A. C. Vutha, D. DeMille, G. Gabrielse, and J. M. Doyle, A cryogenic beam of refractory, chemically reactive molecules with expansion cooling, Phys. Chem. Chem. Phys. 13, 18976 (2011).
- [20] J. Hasted and S. C. Brown, *Physics of Atomic Collisions* (Butterworths, London, 1965).

- [21] N. R. Hutzler, H.-I. Lu, and J. M. Doyle, The buffer gas beam: An intense, cold, and slow source for atoms and molecules, Chem. Rev. **112**, 4803 (2012).
- [22] M. J. Weida and D. J. Nesbitt, Collisional alignment of CO₂ rotational angular momentum states in a supersonic expansion, J. Chem. Phys. 100, 6372 (1994).
- [23] H. Pauly, Atom, Molecule, and Cluster Beams II: Cluster Beams, Fast and Slow Beams, Accessory Equipment and Applications, Vol. 32 (Springer-Verlag, Berlin, Heidelberg, 2000).
- [24] T. Wakabayashi, T. Momose, and M. E. Fajardo, Matrix isolation spectroscopy and spectral simulations of isotopically substituted C₆₀ molecules, J. Chem. Phys. 151, 234301 (2019).
- [25] N. Sogoshi, Y. Kato, T. Wakabayashi, T. Momose, S. Tam, M. E. DeRose, and M. E. Fajardo, High-resolution infrared absorption spectroscopy of C₆₀ molecules and clusters in parahydrogen solids, J. Phys. Chem. A 104, 3733 (2000).
- [26] B. Friedrich, Cold Molecules: Theory, Experiment, Applications (CRC Press Taylor and Francis Group, Boca Raton, FL, 2009).
- [27] C. S. Parmenter, Vibrational energy flow within excited electronic states of large molecules, J. Phys. Chem. **86**, 1735 (1982).
- [28] R. E. Smalley, Vibrational randomization measurements with supersonic beams, J. Phys. Chem. 86, 3504 (1982).
- [29] R. E. Smalley, Dynamics of Electronically Excited States, Annu. Rev. Phys. Chem. 34, 129 (1983).
- [30] D. J. Nesbitt and R. W. Field, Vibrational energy flow in highly excited molecules: Role of intramolecular vibrational redistribution, J. Phys. Chem. 100, 12735 (1996).
- [31] T. Cottrell, *Molecular Energy Transfer in Gases* (Butterworths, London, 1961).
- [32] H. Du, D. J. Krajnovich, and C. S. Parmenter, An experimental exploration of the energy gap law for vibration-translation energy transfer. The I_2^* + M system, J. Phys. Chem. **95**, 2104 (1991).
- [33] A. Sinha, M. C. Hsiao, and F. F. Crim, Bond-selected bimolecular chemistry: H+HOD $(4\nu_{OH}) \rightarrow OD + H_2$, J. Chem. Phys. **92**, 6333 (1990).
- [34] A. Sinha, J. D. Thoemke, and F. F. Crim, Controlling bimolecular reactions: Mode and bond selected reaction of water with translationally excited chlorine atoms, J. Chem. Phys. 96, 372 (1992).
- [35] A. Amirav, U. Even, and J. Jortner, Cooling of large and heavy molecules in seeded supersonic beams, Chem. Phys. **51**, 31 (1980).

- [36] J. T. Stewart, B. E. Brumfield, B. M. Gibson, and B. J. McCall, Inefficient vibrational cooling of C₆₀ in a supersonic expansion, Int. Sch. Res. Notices **2013**, 675138 (2013).
- [37] D. Rapp and T. Kassal, Theory of vibrational energy transfer between simple molecules in nonreactive collisions, Chem. Rev. **69**, 61 (1969).
- [38] R. D. Johnson, G. Meijer, and D. S. Bethune, C₆₀ has icosahedral symmetry, J. Am. Chem. Soc. 112, 8983 (1990).
- [39] R. Taylor, J. P. Hare, A. Abdul-Sada, and H. Kroto, Isolation, separation and characterisation of the fullerenes C_{60} and C_{70} : the third form of carbon, J. Chem. Soc., Chem. Commun., 1423 (1990).
- [40] K. Balasubramanian, Nuclear-spin statistics of C_{60} , $C_{60}H_{60}$ and $C_{60}D_{60}$, Chem. Phys. Lett. **183**, 292 (1991).
- [41] C. Curceanu, J. D. Gillaspy, and R. C. Hilborn, Resource letter SS-1: The spin-statistics connection, Am. J. Phys. 80, 561 (2012).
- [42] O. Greenberg, Particles with small violations of Fermi or Bose statistics, Phys. Rev. D 43, 4111 (1991).
- [43] O. Greenberg, Example of infinite statistics, Phys. Rev. Lett. 64, 705 (1990).
- [44] R. N. Mohapatra, Infinite statistics and a possible small violation of the Pauli principle, Phys. Lett. B **242**, 407 (1990).
- [45] D. I. Fivel, Interpolation between fermi and bose statistics using generalized commutators, Phys. Rev. Lett. 65, 3361 (1990).
- [46] M. D. Angelis, G. Gagliardi, L. Gianfrani, and G. M. Tino, Test of the symmetrization postulate for spin-0 particles, Phys. Rev. Lett. **76**, 2840 (1996).
- [47] R. C. Hilborn and C. L. Yuca, Spectroscopic test of the symmetrization postulate for spin-0 nuclei, Phys. Rev. Lett. 76, 2844 (1996).
- [48] H. Naus, A. De Lange, and W. Ubachs, $b^1\Sigma_{\rm g}^+ {\rm X}^3\Sigma_{\rm g}^-(0,0)$ band of oxygen isotopomers in relation to tests of the symmetrization postulate in $^{16}{\rm O}_2$, Phys. Rev. A **56**, 4755 (1997).
- [49] L. Gianfrani, R. W. Fox, and L. Hollberg, Cavity-enhanced absorption spectroscopy of molecular oxygen, J. Opt. Soc. Am. B 16, 2247 (1999).
- [50] D. Mazzotti, P. Cancio, G. Giusfredi, M. Inguscio, and P. D. Natale, Search for Exchange-Antisymmetric States for Spin-0 Particles at the 10⁻¹¹ Level, Phys. Rev. Lett. **86**, 1919 (2001).
- [51] P. C. Pastor, I. Galli, G. Giusfredi, D. Mazzotti, and P. D. Natale, Testing the validity of Bose-Einstein statistics in molecules, Phys. Rev. A 92, 063820 (2015).
- [52] G. M. Tino, Testing the symmetrization postulate of quantum mechanics and the spin-statistics connection, Fortschr. Phys. 48, 537 (2000).